Inorg. Chem. **2008**, *47*, 1465−1475

Crown Ether Inclusion Complexes of the Early Actinide Elements, $[AnO_2(18\text{-crown-}6)]^{n+}$, An = U, Np, Pu and $n = 1, 2$: A Relativistic Density Functional Study

Grigory A. Shamov,[†] Georg Schreckenbach,[*,†] Richard L. Martin,[‡] and P. Jeffrey Hay[‡]

Department of Chemistry, University of Manitoba, Winnipeg, Manitoba, Canada, R3T 2N2, and Theoretical Division, Mail Stop MS B268, Los Alamos National Laboratory, Los Alamos, New Mexico 87545

Received August 2, 2007

The title compounds, $[AnO_2(18\text{-crown-}6)]^{n+}$, An = U, Np, and Pu and $n = 1$ and 2, as well as the related (experimentally observed) complex $[UO_2(\text{dicyclohexyl-18-crown-}6)]^{2+}$ are studied using relativistic density functional theory (DFT). Different relativistic methods (large-core and small-core effective core potentials, all-electron scalar four-component) and two flavors of approximate DFT (B3LYP and PBE) are used. Calculated bond lengths agree well with the available experimental data for the Np^{V} complex, while larger differences for the U^{VI} complexes appear to be related to the large uncertainties in the experimental data. The axial An═O bonds are found to be weaker and longer than in the corresponding penta-aquo complexes, though still of partial triple-bond character. The An═O bond lengths and strengths decrease along the actinide series, consistent with the actinide contraction. Gas-phase binding energies calculated for the penta-aquo complexes and crown-ether complexes of the actinides studied, as well as ligand-exchange energies, show that there is no intrinsic preference, or "better fit", for actinyl(V) cations as compared to actinyl(VI) ones. Rather, the ability of NpO_2^{+} (Np^{V}) to form in-cavity 18-crown-6 complexes in water, which is impossible for UO_2^{2+}, is traced to solvation effects in polar solvents. Thus, the experimentally observed stabilization of the pentavalent oxidation state as compared to the hexavalent one is due to the effective screening of the charge provided by the macrocycle, and this leads to destabilization of the An^{VI} crown complexes relative to their An^{V} counterparts.

Introduction

The chemistry of the early actinide elements thorium through americium has importance from both fundamental and practical standpoints.[1] The role of relativistic and electron correlation effects as well as the participation of 6d and 5f shells not available elsewhere in the periodic table present fundamental issues regarding the bonding and electronic structure of actinide complexes.[2] Practical considerations arise from the use of actinides in nuclear energy and nuclear materials where such issues as long-term storage of nuclear waste, environmental cleanup, and actinide separations need to be addressed.

One of the methods proposed for nuclear waste treatment and actinide separation involves the coordination of actinide ions with polydentate macrocyclic ligands, thus exploiting the chelate effect.[3] These systems are attractive because they could potentially be tuned to provide a specific fit to the target metal by changing the size of the respective cavity. Other parameters that can be varied in principle include the nature of the donor atoms, steric requirements, or details of the electronic structure of the complex such as ligand aromaticity.

Actinide inclusion complexes of macrocycles that have been studied experimentally include, among others, expanded

* Author to whom correspndence should be addressed. E-mail: schrecke@cc.umanitoba.ca.
† University of Manitoba.
‡ Los Alamos National Laboratory.

(1) Morss, L. R.; Edelstein, N. M.; Fuger, J.; Katz, J. J. *The Chemistry of the Actinide and Transactinide Elements*, 3rd ed.; Springer: Berlin, NY, 2006.
(2) Kaltsoyannis, N.; Scott, P. *The F Elements*; Oxford University Press: New York, 1999.
(3) Gorden, A. E. V.; Xu, J.; Raymond, K. N.; Durbin, P. *Chem. Rev.* **2003**, *103*, 4207.

10.1021/ic7015403 CCC: $40.75
Published on Web 01/29/2008

porphyrin systems[4–6] and related macrocycles with Schiff-base donor atoms;[7,8] calixarenes;[9–13] and crown ethers,[13–17] aza-crowns,[13] and boron-containing macrocycles.[18]

On the theoretical side, there has not been comparable activity in studying such complexes. This is likely due to the size of these systems, combined with the inherent challenges of performing meaningful calculations on f-element species.[19–23] Cao and Dolg[24] have studied complexes between lanthanide ions and the tripyrrolic, penta-aza texaphyrin ligand, one of many expanded porphyrins. Liao et al.[25] have used relativistic density functional theory (DFT) to investigate the actinyl(VI) complexes formed with the alaskaphyrin ligand but using an idealized geometry. Very recently, Cao et al.[26] published a study of Ln^{III} and An^{III} complexes formed with the five-donor motexafin ligand. We are not aware of any other first-principle computational study of such complexes published to date, apart from our own work[27,28] that includes a preliminary report on the systems that are the subject of the present article.[29]

Further regarding the experimental results, Clark et al.[17] have reported the synthesis of a complex in which the neptunyl(V) ion NpO_2^{1+} is encapsulated by the 18-crown-6 ligand. They were able to crystallographically characterize the ion in the form of the $[NpO_2(18\text{-crown-}6)]ClO_4$ salt. The crystal structure shows six approximately coplanar crown ether oxygen donor atoms coordinated to the central neptunyl ion. While the $[UO_2(18\text{-crown-}6)]^{2+}$ species had been synthesized and characterized previously,[15,16] this is the first example of a transuranic crown ether inclusion complex. We note the experimental preference for the Np^V system over Np^{VI}, the reason of which is not fully understood, although some speculations about size and fit/misfit effects have been made. We also note "*the relative ease of encapsulation (of* $NpO_2]^{1+}$*) in aqueous solution* [that] *contrasts with the related* $[UO_2]^{2+}$ *ion for which anhydrous conditions are necessary to ensure that the crown ether oxygen atoms bind directly to the metal center*" (quoted from ref 17). Thus, the crown ether ligand may have the potential of being an effective system for separation of radioactive fission products, particularly the pertinent actinides.

The only explanation for the differences in the behavior of U^{VI} and Np^V offered in the original experimental work was a simple steric argument about the better fit of the larger neptunyl(V) cation into the inner cavity of the ligand. However, the knowledge available on the complexation of the alkali-metal cations with crown ethers does not always support this simple *fit/misfit* picture.[30] As part of an ongoing research project into elucidating the nature of binary complexes between early actinides and various macrocycles,[27–29] we report here calculations on the title compounds $[AnO_2(18\text{-crown-}6)]^{n+}$, An = U, Np, and Pu and n = 1 and 2. For comparison with the experiment available,[15,16] we also consider the uranyl(VI) complex of the bis-dicyclohexylo-18-crown-6 ligand. Our study was originally motivated by the mentioned work of Clark et al.,[17] as well as by the prospect of similar chemistry involving the element plutonium. Preliminary results, at the time using the—now outdated—large-core effective core potentials (LC-ECP) method (see the section "Computational Details" below), have been published previously.[29]

Computational Details

All calculations were based on relativistic DFT. To date, DFT[31] is effectively the only practical choice for medium-to-large actinide molecules.[21–23] We use two flavors of approximate DFT, the hybrid functional B3LYP[32–34] and the "generalized gradient approximation" (GGA) functional PBE.[35] We have extensively tested the choice of approximate DFT as applied to actinide molecules.[36–38] In a nutshell, GGA functionals such as PBE gave the best bond

(4) Sessler, J. L. *Expanded, Contracted and Isomeric Porphyrins*; Pergamon Press: New York, 1997.
(5) Sessler, J. L.; Vivian, A. E.; Seidel, D.; Burrell, A. K.; Hoehner, M.; Mody, T. D.; Gebauer, A.; Weghorn, S. J.; Lynch, V. *Coord. Chem. Rev.* **2001**, *216–217*, 411.
(6) Sessler, J. L.; Gorden, A. E. V.; Seidel, D.; Hannah, S.; Lynch, V.; Gordon, P. L.; Donohoe, R. J.; Tait, C. D.; Keogh, D. W. *Inorg. Chim. Acta* **2002**, *341*, 54.
(7) Sessler, J. L.; Mody, T. D.; Lynch, V. *Inorg. Chem.* **1992**, *31*, 529.
(8) Sessler, J. L.; Mody, T. D.; Dulay, M. T.; Espinoza, R.; Lynch, V. *Inorg. Chim. Acta* **1996**, *246*, 23.
(9) Thuéry, P.; Nierlich, M. *J. Inclusion Phenom. Macrocyclic Chem.* **1997**, *27*, 13.
(10) Thuéry, P.; Nierlich, M.; Masci, B.; Asfari, Z.; Vicens, J. *J. Chem. Soc., Dalton Trans.* **1999**, 3151.
(11) Thuéry, P.; Nierlich, M.; Vicens, J.; Masci, B.; Takemura, H. *Eur. J. Inorg. Chem.* **2001**, 637.
(12) Thuéry, P.; Nierlich, M.; Vicens, J.; Masci, B. *J. Chem. Soc., Dalton Trans.* **2001**, 867.
(13) Thuéry, P.; Keller, N.; Lance, M.; Vigner, J.-D.; Nierlich, M. *New J. Chem.* **1995**, *19*, 619.
(14) Rogers, R. D.; Bond, A. H.; Hipple, W. G.; Rollins, A. N.; Henry, R. F. *Inorg. Chem.* **1991**, *30*, 2671.
(15) Navaza, A.; Villain, F.; Charpin, P. *Polyhedron* **1984**, *3*, 143.
(16) Deshayes, L.; Keller, N.; Lance, M.; Navaza, A.; Nierlich, M.; Vigner, J. *Polyhedron* **1994**, *13*, 1725.
(17) Clark, D. L.; Keogh, D. W.; Palmer, P. D.; Scott, B. L.; Tait, C. D. *Angew. Chem., Int. Ed. Engl.* **1998**, *37*, 164.
(18) Barnea, E.; Andrea, T.; Kapon, M.; Eisen, M. S. *J. Am. Chem. Soc.* **2004**, *126*, 5066.
(19) Pepper, M.; Bursten, B. E. *Chem. Rev.* **1991**, *91*, 719.
(20) Dolg, M. In *Encyclopedia of Computational Chemistry*; Schleyer, P. R. v., Ed.; Wiley Interscience: New York, 1998.
(21) Schreckenbach, G.; Hay, P. J.; Martin, R. L. *J. Comput. Chem.* **1999**, *20*, 70.
(22) Kaltsoyannis, N. *Chem. Soc. Rev.* **2003**, *32*, 9.
(23) Vallet, V.; Macak, P.; Wahlgren, U.; Grenthe, I. *Theor. Chem. Acc.* **2006**, *115*, 145.
(24) Cao, X. Y.; Dolg, M. *Mol. Phys.* **2003**, *101*, 2427.
(25) Liao, M.-S.; Kar, T.; Scheiner, S. *J. Phys. Chem. A* **2004**, *108*, 3056.
(26) Cao, X. Y.; Li, Q. S.; Moritz, A.; Xie, Z. Z.; Dolg, M.; Chen, X. B.; Fang, W. H. *Inorg. Chem.* **2006**, *45*, 3444.
(27) Shamov, G. A.; Schreckenbach, G. *J. Phys. Chem. A* **2006**, *110*, 9486.
(28) Shamov, G. A.; Schreckenbach, G. *Inorg. Chem.* [Online early access]. DOI: 10.1021/ic701192t. Published Online: Jan 9, 2008.
(29) Martin, R. L.; Hay, P. J.; Schreckenbach, G. In *Plutonium Futures - the Science: Topical Conference on Plutonium and the Actinides, AIP Conference Proceedings 532*; Pilay, K. K. S., Kim, K. C., Eds.; American Institute of Physics: College Park, Maryland, 2000; pp 392.
(30) Gokel, G. W.; Leevy, W. M.; Weber, M. E. *Chem. Rev.* **2004**, *104*, 2723.
(31) Koch, W.; Holthausen, M. C. *A Chemist's Guide to Density Functional Theory*; Wiley Verlag Chemie: New York, 2000.
(32) Becke, A. D. *J. Chem. Phys.* **1993**, *98*, 5648.
(33) Lee, C.; Yang, W.; Parr, R. G. *Phys. Rev. B: Condens. Matter Mater. Phys.* **1988**, *37*, 785.
(34) Stephens, P. J.; Devlin, F. J.; Chabalowski, C. F.; Frisch, M. J. *J. Phys. Chem.* **1994**, *98*, 11623.
(35) Perdew, J. P.; Burke, K.; Ernzerhof, M. *Phys. Rev. Lett.* **1996**, *77*, 3865.
(36) Batista, E. R.; Martin, R. L.; Hay, P. J.; Peralta, J. E.; Scuseria, G. E. *J. Chem. Phys.* **2004**, *121*, 2144.
(37) Shamov, G. A.; Schreckenbach, G. *J. Phys. Chem. A* **2005**, *109*, 10961; correction note: ibid. **2006**, *110*, 12072.

lengths and vibrational frequencies, whereas hybrid functionals such as B3LYP resulted in superior energetics (reaction enthalpies, bond dissociation energies, and the like). For the An^{VI}/An^{V} reduction potential in the aquo complexes $[An(H_2O)_5]^{n+}$, however, we did not find a clear advantage for either hybrid functionals or GGAs.[37] In general, different choices for GGA functionals gave essentially similar results. Likewise, comparing different hybrid functionals did not reveal any major differences in performance.[38]

The calculations were performed with two different quantum-chemical codes, Gaussian 03[39] (G03) and Priroda.[40–43]

In Gaussian, we use relativistic ECP to describe scalar relativistic effects. The older LC-ECPs include 78 electrons in the core of the actinide metal,[44] leaving 14 (U), 15 (Np), or 16 (Pu) valence electrons. (These are the ECPs that have been used in our preliminary report[29] on the title complexes.) More recently, evidence has been mounting that small-core ECPs[45] (SC-ECPs)—that include only 60 electrons in the core—yield much higher accuracy for about any given property.[36,37,46–48] Thus, we use SC-ECPs for production calculations but provide some LC-ECP results for reference purposes.

In Gaussian calculations, we use the following basis sets. In LC-ECP calculations, we represent the actinide metal by the respective basis sets as published.[44] For SC-ECP calculations, we took the SDD actinide basis sets corresponding to the SC-ECPs,[45] as obtained from the EMSL library,[49] and removed the most diffuse s, p, d, and f functions. These basis sets were used in a completely uncontracted form ("split SC-ECP basis"). Such modification of the basis allows for avoiding linear dependence in the basis set and achieving better stability and speed of the SCF procedure. For comparison, we have also done some calculations with the original contracted form. For ligand atoms, the standard 6-31G(d) basis sets were used. Following earlier studies (e.g., refs 50 and 51), we use "ultrafine" integration grids to ensure numerical accuracy and stability. In those cases where the formal metal occupation suggests an open-shell metal configuration, we solved for the high-spin state in an unrestricted Kohn–Sham approximation. Most of the Gaussian calculations were done using the hybrid B3LYP density functional. For the sake of direct comparison with Priroda calculations (which are described below), we did PBE SC-ECP calculations for the case of the uranyl(VI) crown complex as well.

The Priroda code applied by us[40–43] takes an all-electron (AE) approach to the relativistic problem.[38,42] Contrary to two-component approximations such as Douglas−Kroll or zeroth-order regular approximation, this AE method is based on the full, four-component one-electron Dirac equation with spin–orbit effects separated out[52] and neglected in a scalar relativistic approximation. This leaves a large and a small component of the wave function. The code uses energy-optimized Gaussian basis sets for the large component, and the corresponding kinetically balanced basis for the small component.[43] In the present calculations, we use extensive large-component basis sets of triple-ζ polarized (L2) quality. The contractions are (8,4,2)/[3,2,1] for hydrogen, (12,8,4,2)/[4,3,2,1] for carbon and oxygen, and (37,36,27,21,10,5)/[13,12,10,7,3,1] for the actinides. Priroda makes judicious use of the "resolution-of-identity" approach[40,42] to solving the SCF equations, as well as other efficiency-enhancing techniques. Overall, these features make the code extremely efficient.

We have extensively tested[27,37,38] the validity and reliability of the (relativistic) methods available in Priroda in application to actinide compounds. All modern methods (including AE and SC-ECP) were shown by us to yield similar results provided that all the other settings (XC functional or correlation treatment, respectively; reasonably converged basis sets; accurate numerical integration) are comparable. Thus, we will combine the Priroda results with results from SC-ECP calculations for the purpose of treating solvation effects as described below.

Solvent effects are included using the conductor-like polarizable continuum model (CPCM)[53] as implemented in the Gaussian code.[39] The dielectric constant for the water solvent was taken as 78.4. While studying the actinyl water system $[AnO_2(H_2O)_5]^{n+}$, An = U, Np, and Pu and n = 1 and 2, we have recently tested continuum solvation models in a detailed comparison to cluster models that contain explicit water molecules in the second coordination sphere, as well as mixed cluster-continuum models explicitly including the second coordination sphere of the actinyls.[37] We have found that single-point calculations on gas-phase geometries are sufficient for energetics. Reoptimization in the presence of the solvent, while important for (equatorial) bond lengths, was found to have a minor influence on energetics.[37] Thus, the single-point approach has been employed in the current study, for it allows minimizing computational costs without sacrificing much accuracy in solvation energies.

It should be noted that continuum solvation models, being parametrized methods, yield solvation energies that depend strongly on the detailed parameters of the model used, notably the size and shape of the solvent-excluded cavity.[37,54] In particular, the conductor-like screening model (COSMO; Klamt and Schüürmann[55]) radii parametrization yields solvation energies markedly different from those of the united atom (UA0) model widely used in the CPCM implementation in the Gaussian 03 program.[39] Some benchmark studies hint to the former being the superior.[37,54] In the present work, we apply both the default CPCM method and the COSMO radii.

In principle, one can select, especially for the actinyl aquo complexes, several models that differ in the degree of explicitly including the solvation shells of the ion: to include only the ion, the ion and its first coordination shell, the ion and its first and second shells, and so forth. Inclusion of a bare actinyl is possible but would require reparametrization of the continuum model. Inclusion of the shells beyond the first one, besides being computationally very demanding, has its own severe methodological problems[37]—manifolds of closely lying isomers requiring dynamical simulation, accuracy considerations of the QM method itself, and so forth.

In our earlier work on the hydration of the actinyls ions,[37] we found that solvation effects are represented accurately enough by

(38) Shamov, G. A.; Schreckenbach, G.; Vo, T. *Chem.—Eur. J.* **2007**, *13*, 4932.
(39) Frisch, M. J. et al. *Gaussian 03*; Gaussian, Inc.: Wallingford, CT, 2004.
(40) Laikov, D. N. *Chem. Phys. Lett.* **1997**, *281*, 151.
(41) Laikov, D. N. *Priroda Code*, version 5; Moscow State University: Moscow, 2004.
(42) Laikov, D. N.; Ustynyuk, Y. A. *Russ. Chem. Bull.* **2005**, *54*, 820.
(43) Laikov, D. N. *Chem. Phys. Lett.* **2005**, *416*, 116.
(44) Hay, P. J.; Martin, R. L. *J. Chem. Phys.* **1998**, *109*, 3875.
(45) Küchle, W.; Dolg, M.; Stoll, H.; Preuss, H. *J. Chem. Phys.* **1994**, *100*, 7535.
(46) Han, Y.-K.; Hirao, K. *J. Chem. Phys.* **2000**, *113*, 7345.
(47) Han, Y. K. *J. Comput. Chem.* **2001**, *22*, 2010.
(48) Schreckenbach, G. *Int. J. Quantum Chem.* **2005**, *101*, 372.
(49) *Gaussian Basis Set Order Form*. http://www.emsl.pnl.gov/forms/basisform.html (accessed Jan 2007).
(50) Schreckenbach, G. *Inorg. Chem.* **2000**, *39*, 1265.
(51) Schreckenbach, G.; Hay, P. J.; Martin, R. L. *Inorg. Chem.* **1998**, *37*, 4442.
(52) Dyall, K. G. *J. Chem. Phys.* **1994**, *100*, 2118.
(53) Cossi, M.; Rega, N.; Giovanni, S.; Barone, V. *J. Comput. Chem.* **2003**, *24*, 669.
(54) Gutowski, K. E.; Dixon, D. A. *J. Phys. Chem. A* **2006**, *110*, 8840.
(55) Klamt, A.; Schüürmann, G. *J. Chem. Soc., Perkin Trans.* **1993**, *2*, 799.

Table 1. Selected Calculated and Experimental Bond Lengths (Å) and Uranyl Frequencies (cm^{-1}) for the Uranium(VI) Crown Complexes

	18-crown-6 complexes						fused crown[a]	fused crowns[b]	
	LC-ECP, B3LYP	SC-ECP, B3LYP	split SC-ECP, B3LYP	split SC-ECP, PBE	AE/L2, PBE	exptl.[c]	AE/L2, PBE[a]	exptl.[b]	
R U═O (axial)	1.763	1.757	1.756	1.777	1.776	1.63(5)	1.779	1.77(4)	*1.75(3)*
	1.763	1.757	1.756	1.777	1.776	1.64(4)	1.779	1.77(4)	*1.82(3)*
R U−O (equatorial)	2.598	2.575	2.576	2.566	2.569	2.44(5)	2.532	2.43(4)	*2.46(4)*
	2.598	2.575	2.576	2.566	2.570	2.47(4)	2.532	2.44(4)	*2.54(5)*
	2.601	2.579	2.579	2.573	2.578	2.49(4)	2.534	2.46(4)	*2.59(4)*
	2.601	2.579	2.579	2.573	2.578	2.52(5)	2.568	2.48(4)	*2.60(4)*
	2.602	2.581	2.581	2.573	2.578	2.53(5)	2.621	2.56(4)	*2.63(6)*
	2.602	2.581	2.581	2.575	2.578	2.55(5)	2.622	2.68(4)	*2.68(5)*
average equatorial[d]	2.600	2.578	2.579	2.571	2.575	2.50	2.568	2.51	*2.58*
ν AnO_2 symm		930	929	856; 882	850; 877		856		
ν AnO_2 asymm		1013	1011	954	952		941		

[a] Dicyclohexyl-fused crown ether complex $[UO_2$(dicyclohexyl-18-crown-6)$]^{2+}$; see Figure 2 and the text. [b] UO_2(dicyclohexyl-18-crown-6)·$(ClO_4)_2$ and UO_2(dicyclohexyl-18-crown-6)·$(CF_3SO_3)_2$ (*second number; italic*).[15,16] [c] Experimental data from Deshayes et al.[16] [d] Arithmetic average.

a model containing the metal and its first coordination sphere embedded into a continuum model with a "standard" atomic radii parametrization for the remainder of the solvent. Thus, we chose this model for the present work for studying both the actinyl aquo and crown ether complexes.

Moreover, an entropy correction has to be applied to the free energy of those reactions that result in forming or consuming of a water molecule.[56] This correction accounts for the reduction in translational entropy of a water molecule solvated in water (relative to the standard state). Following earlier studies,[56] this is done by setting the water pressure to 1354 atm (value derived from a liquid water density of 997.02 kg/m^3) instead of 1 atm. At 298 K, this would contribute −4.3 kcal/mol in Gibbs free energy of any reaction involving water, per single water molecule. We have shown[37] that this approach gives reliable results for reactions containing solvated actinide complexes. For the cluster calculations involving a cluster $(H_2O)_n$, we had neglected these corrections. The correction in this case would be *at most* $-4.3/n$ kcal/mol, where n is the number of water molecules in the cluster—an error that is much smaller than other uncertainties of the models.[37]

As the current version of the Priroda code does not contain any continuum solvation models, we have obtained solvation energies $\Delta\Delta G^{solv}$ from G03-based single-point solvation calculations, using both the CPCM and COSMO radii. These calculations employed the Priroda optimized AE/L2 gas-phase PBE geometries, the PBE density functional, and the SC-ECP basis set combination described above. As noted above, we have used this procedure successfully previously;[37] solvation energies $\Delta\Delta G^{solv}$ were found to be sensitive to the solvation model used (especially the radii for the solvent-excluded cavities) but relatively insensitive to the accompanying gas-phase model chemistry.

All calculations were performed using the scalar relativistic approximation, that is, neglecting spin–orbit effects. For structures and frequencies, this is thought to be a reasonable approximation. We note that, for energetics involving a change in the number of unpaired f electrons, this would introduce an appreciable error.

Geometry optimizations with either G03 or Priroda have been performed without any symmetry or other constraints. Optimized geometries are always verified as minima on the potential energy surface by calculating the harmonic vibrational frequencies at the stationary point, analytically in the case of Gaussian and numerically with the Priroda code. Anharmonic effects on the frequencies have not been considered. The calculated frequencies are also used for the thermochemistry.

Table 2. Selected Calculated Bond Lengths (Å) and Uranyl Frequencies (cm^{-1}) for the Uranium(V) Complex $[UO_2$(18-crown-6)$]^{1+}$

	LC-ECP, B3LYP	SC-ECP, B3LYP	split SC-ECP, B3LYP	AE/L2, PBE
R U═O (axial)	1.810	1.818	1.819	1.820
	1.810	1.818	1.819	1.820
R U−O (equatorial)	2.667	2.654	2.654	2.640
	2.668	2.654	2.654	2.640
	2.708	2.686	2.684	2.688
	2.708	2.686	2.684	2.688
	2.717	2.686	2.684	2.689
	2.718	2.686	2.684	2.689
average equatorial[a]	2.698	2.675	2.674	2.672
ν AnO_2 symm		834	830	800
ν AnO_2 asymm		898	893	854

[a] Arithmetic average.

Atomic charges (Hirshfeld[57]), spin densities,[57] and population (Mayer) bond orders[58] have been calculated at the AE/L2 PBE level of theory. Experience shows that the Hirshfeld charges, while smaller than, for instance, the Mulliken charges, give a chemically meaningful picture in that they change in a reasonable way with molecular structure changes. Likewise, the population (Mayer) bond orders, while to some degree basis-set-dependent, give bond orders and trends in bond orders that are consistently in agreement with intuitive chemical models for various actinide complexes.[27,38,59,60]

Finally, we have to note that one data point (G03-SC-ECP-B3LYP gas-phase calculation on $[PuO_2$(18-crown-6)$]^{2+}$) in our hands failed to obtain a stable SCF solution, yielding instead a solution corresponding to an electronically excited state, probably involving certain configurations of the f electrons at the plutonyl. We excluded the point for that reason. Also, due to some errors in the G03 code, solvation calculations for the U^V crown complex using the GGA PBE functional failed, so we take the solvation energies of that complex from the corresponding complex of neptunyl(V), which should not be significantly different.

Results and Discussion

1. Geometries. Optimized geometries (axial and equatorial U−O bond lengths) of the 18-crown-6 complexes of UO_2^{2+} and UO_2^{1+} are provided in Tables 1 and 2, respectively. We have also included the symmetric and antisymmetric uranyl

(56) Martin, R. L.; Hay, P. J.; Pratt, L. R. *J. Phys. Chem. A* **1998**, *102*, 3565.
(57) Hirshfeld, F. L. *Theor. Chim. Acta* **1977**, *44*, 129.
(58) Mayer, I. *Simple Theorems, Proofs, and Derivations in Quantum Chemistry*; Kluwer Academic/Plenum Publishers: New York, 2003.
(59) Berard, J. J.; Shamov, G. A.; Schreckenbach, G. *J. Phys. Chem. A* **2007**, *101*, 10789.
(60) Namdarghanbari, M. A.; Shamov, G. A.; Schreckenbach, G. *J. Am. Chem. Soc.* **2008**, submitted.

Table 3. Selected Calculated and Experimental Bond Lengths (Å) and Neptunyl Frequencies (cm^{-1}) for the Neptunium(Vi) and (V) Complexes

	$[NpO_2(18\text{-crown-6})]^{2+}$			$[NpO_2(18\text{-crown-6})]^{1+}$			
	LC-ECP, B3LYP	split SC-ECP, B3LYP	AE/L2, PBE	LC-ECP, B3LYP	split SC-ECP, B3LYP	AE/L2 PBE	exptl.[a]
R Np=O (axial)	1.759	1.736	1.757	1.810	1.795	1.806	1.800(5)
	1.759	1.736	1.757	1.809	1.795	1.806	1.800(5)
R Np−O (equatorial)	2.588	2.560	2.553	2.665	2.645	2.635	2.576(9)
	2.588	2.561	2.553	2.672	2.647	2.647	2.576(9)
	2.603	2.577	2.582	2.701	2.681	2.679	2.603(8)
	2.603	2.579	2.582	2.705	2.681	2.680	2.603(8)
	2.609	2.579	2.583	2.712	2.682	2.688	2.604(10)
	2.609	2.580	2.583	2.715	2.682	2.689	2.604(10)
average equatorial[b]	2.600	2.573	2.573	2.695	2.670	2.670	2.594
ν AnO_2 symm	839	926	848	776	835	791	780
ν AnO_2 asymm	952	1021	955	877	911	866	

[a] Clark et al.[17] [b] Arithmetic average.

Table 4. Selected Calculated Bond Lengths (Å) and Plutonyl Frequencies (cm^{-1}) for the Plutonium(VI) and (V) Complexes

	$[PuO_2(18\text{-crown-6})]^{2+}$		$[PuO_2(18\text{-crown-6})]^{1+}$		
	LC-ECP, B3LYP	AE/L2, PBE	LC-ECP, B3LYP	split SC-ECP, B3LYP	AE/L2, PBE
R Pu=O (axial)	1.780	1.753	1.809	1.776	1.789
	1.780	1.753	1.809	1.776	1.789
R Pu−O (equatorial)	2.588	2.562	2.664	2.650	2.639
	2.597	2.562	2.665	2.651	2.639
	2.599	2.580	2.693	2.679	2.676
	2.599	2.581	2.694	2.679	2.676
	2.605	2.581	2.695	2.679	2.677
	2.605	2.582	2.704	2.679	2.677
average equatorial[a]	2.599	2.575	2.686	2.670	2.664
ν AnO_2 symm		829		818	784
ν AnO_2 asymm		943		908	868

[a] Arithmetic average.

stretching frequencies for these molecules. The corresponding results for Np and Pu are collected in Tables 3 and 4. As an example, we show in Figure 1 the SC-ECP-B3LYP optimized geometry of the experimentally observed[17] Np^V complex. The AE/L2 PBE method results in structures that are qualitatively very similar, having a saddle-type bent macrocyclic ligand with all six oxygens coordinating to the actinide atom. Likewise, the Np^{VI}, U^V, U^{VI}, Pu^V, and Pu^{VI} complexes possess qualitatively similar geometries as well.

Comparing first the LC-ECP[29] and SC-ECP results for the five complexes where we have been able to obtain results, we note that the calculated equatorial bond lengths are shorter by about 0.02−0.03 Å for the latter. The SC-ECP-calculated equatorial bond lengths are closer to experimental results than the LC-ECP ones (see below). This trend is consistent with results for other systems such as the aquo complexes $[AnO_2(H_2O)_5]^{n+}$, An = U, Np, and Pu and n = 1 and 2, where the shorter equatorial bond lengths of the SC-ECP approach led to markedly better agreement with experimental results.[37,61] Axial (actinyl An=O) bond lengths are also predicted to be systematically shorter for SC-ECP as compared to LC-ECP in all cases except U^V, which *may* be due to a problem with the older LC-ECP calculations.

The basis set contraction scheme for the ECP calculations (completely uncontracted SC-ECP basis versus the original contracted basis for the metal) has been tested for the uranium(VI) and (V) complexes, Tables 1 and 2. We note that the differences between the two sets of results are marginal for both bond lengths and uranyl frequencies.

We note that our earlier detailed comparisons of different density functionals, namely, hybrid and pure GGA DFT, had shown that hybrid DFT methods tend to predict shorter axial U=O and equatorial U−X bonds than GGA.[37,38] The current AE-PBE results follow the trend, Tables 1−4. Especially for the axial bonds, they predict bond distances that are longer than those of SC-ECP-B3LYP by almost 0.03 Å. Equatorial distances in the current AE/L2-PBE results, however, are always *shorter* than those of SC-ECP-B3LYP. This apparent contradiction with the earlier observations can be understood as follows. Equatorial U−O lengths are influenced not only by the character of the U−O bond itself but also by the conformation of the crown ether ligand. Both factors are affected by a change in functional (GGA functionals such as PBE tend to have smaller barriers for conformational changes in the free ether as compared to B3LYP,[31] thus allowing the ligand to be more flexible) and differences in the basis set (L2 is much larger than 6-31G(d) as used for ligands in SC-ECP).

We have reoptimized the uranyl(VI) crown ether complex calculated with the SC-ECP relativistic method combined with the same PBE density functional as used in AE calculations. The structure shows no significant difference with the AE/L2 PBE results; it also yields longer axial and shorter equatorial uranium-to-oxygen distances as compared to the SC-ECP B3LYP optimized structure (Table 1).

(61) Hay, P. J.; Martin, R. L.; Schreckenbach, G. *J. Phys. Chem. A* **2000**, *104*, 6259.

Experimental crystal structures are available for the uranium(VI) and neptunium(V) cases.[15–17] We will start with the U^{VI} case, Table 1, and first discuss the available experimental data before comparing these data to our calculations. Crystal structures for crown ether inclusion complexes of uranyl(VI) have been obtained in three cases. These systems are UO_2(18-crown-6)•$(CF_3SO_3)_2$,[16] UO_2(dicyclohexyl-18-crown-6)•$(ClO_4)_2$,[15] and UO_2(dicyclohexyl-18-crown-6)•$(CF_3SO_3)_2$.[16] All of these structural determinations, while proving the insertion of the uranyl moiety into the ligand cavity, "*suffer from a lack of accuracy in the positions of the light atoms*" (quoted from ref 15). The large experimental error bars (Table 1) are an indication of that. Likewise, differences in experimental uranium-to-ligand bond distances between the triflate complex of the dicyclohexyl-fused crown ligand[16] and the respective perchlorate complex[15] (data shown in Table 1) are very large—the uranyl and average equatorial bond distances are 1.75/1.82 Å and 2.58 Å for the former but 1.77 and 2.51 Å for the latter.

Two of the three experimental structures contain the dicyclohexyl-18-crown-6 ligand (that has two fused cyclohexyl rings on the outside of the crown ether ring) instead of the unsubstituted 18-crown-6 system. We have therefore obtained theoretical structures for the $[UO_2$(dicyclohexyl-18-crown-6)$]^{2+}$ complex as well, using the AE/L2-PBE method. The optimized structure of this complex is shown in Figure 2, and we have included key geometry parameters in Table 1. For the fused rings, there are, in principle, different conformations possible. Indeed, the crystal structure of the outer-sphere uranyl complex that contains uncomplexed dicyclohexyl-18-crown-6 shows two conformations of the ring system. The authors speculate that conformational variations might be one reason for the disorder (and consequently the low resolution) found in the crystal structures of the metal complexes.[15] However, since the cyclohexyl rings are peripheral to the complex, these conformational changes are not expected to have a major influence on the metal-to-ligand bonding in these systems. We have not attempted to sample the entire conformational space of these systems or to locate the global energy minimum. Qualitatively, we note that the calculations reproduce the experimentally observed[15] propeller-shaped form of the 18-crown-6 rings, Figure 2.

The experimental uranyl distances for the unsubstituted complex, 1.63(5) and 1.64(4) Å appear rather short, and they are not supported by our calculations. Moreover, the two structures for the fused crown systems show much longer actinyl bond distances that are also more in line with the neptunyl(V) complex (Table 3; the neptunyl(V) complex will be discussed in more detail next). The AE/L2-PBE calculations on the fused crown complex give uranyl distances that are within the experimental error bar for either measurement. This level of accuracy is also in line with our experience for other actinyl systems.[27,37] We note, in addition, that the calculations predict only a minor increase in the uranyl bond lengths of 0.003 Å in going from the unsubstituted to the fused crown ether ligand. This would be in line with chemical intuition but contradicts the older experimental data[16] for the unsubstituted 18-crown-6 ligand.

Calculated equatorial bond lengths appear to be slightly overestimated as compared to experimental results—although, as pointed out before, the experimental error bars preclude definitive conclusions in this case. For the fused crown complex, in particular, we observe quantitative agreement with the (average) calculated equatorial bond lengths for one set of experimental data but not for the other. One should note that the calculations reported in Table 1 refer to the gas phase. Previously, we found that condensed-phase effects (solvent or crystal packing) might have an influence on the equatorial bond lengths.[37]

As mentioned before, $[NpO_2]^{1+}$ is the only other actinyl system apart from $[UO_2]^{2+}$ that has been encapsulated by a crown ether ligand. An experimental crystal structure is known for NpO_2(18-crown-6)•ClO_4, and this structure appears to be much better resolved than the older uranyl structures discussed before; moreover, vibrational spectra were measured for this compound.[17] Calculated and experimental bond distances and actinyl stretching frequencies are provided in Table 3.

All three methods considered (AE/L2-PBE, SC-ECP-B3LYP, and LC-ECP-B3LYP calculations) result in axial (neptunyl) bond lengths that are within 0.01 Å of the experimental value. The SC-ECP-B3LYP bond length is again the shortest. This, together with the respective vibrational frequencies (see below), indicates an overestimation of the strength of this bond. The equatorial bond lengths are again overestimated by all of our gas-phase calculations. The AE/L2 PBE and SC-ECP-B3LYP approaches give shorter equatorial distances than LC-ECP-B3LYP, as for uranium complexes. A very similar picture is observed for the geometries of plutonyl complexes where no experimental data are available (Table 4).

We will now consider all six An^{VI}/An^{V} species together, Tables 1−4. In going from U to Np to Pu, we notice a strong decrease in axial (actinyl) bond lengths for both the An^{VI} and An^{V}species. This is consistent with the actinide contraction, that is, the contraction and decrease in energy of the 5f orbitals (to the point that eventually, beyond Am or so, they do not participate in bonding anymore.[1,2]) These types of periodic trends are present in other actinyl species also, for instance, the actinyl aquo complexes $[AnO_2(H_2O)_5]^{n+}$[37] (see also below and Table 5). For the average equatorial bond lengths, we see only a slight contraction. Using the same argument regarding the actinide contraction, this can be seen as a result of the dependence of the equatorial bond lengths on both the radii of actinide metals as well as on steric considerations of the ligand ring.

Comparing the An^{VI} and An^{V} species, we see much longer axial and equatorial bond lengths for the latter as compared to the former. This is readily understandable from the metal charges in either case, see below.

It is instructive to compare the calculated bond lengths to the actinyl aquo complexes $[AnO_2(H_2O)_5]^{n+}$.[37] Because in our previous study[37] we had applied slightly different basis sets, we have recalculated the penta-aquo complexes

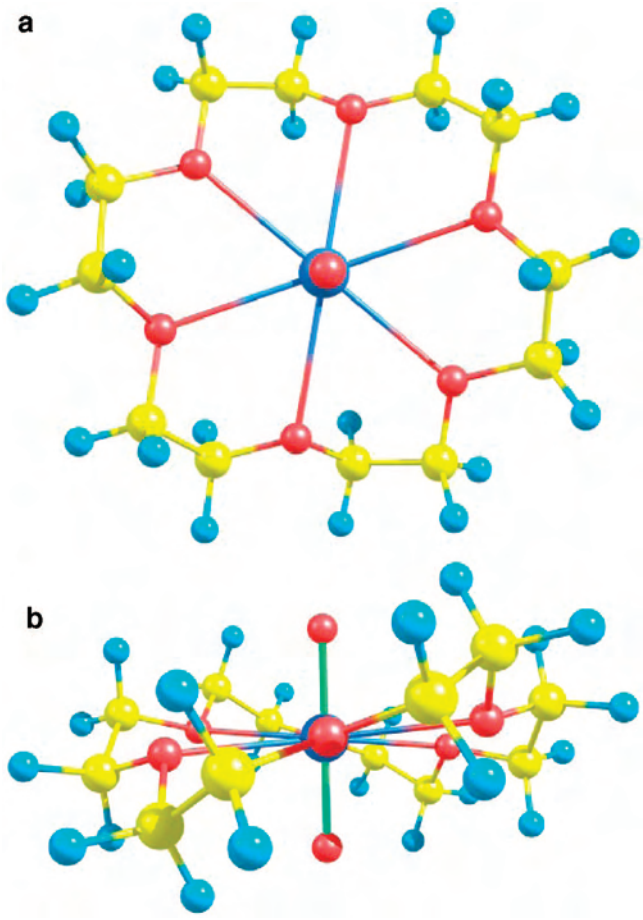

Figure 1. Optimized structure (SC-ECP-B3LYP) of the neptunyl(V) complex $[NpO_2(18\text{-crown-6})]^{1+}$, top (a) and side views (b).

with the AE/L2 PBE method and other settings, as used throughout the present paper. The relevant data are presented in Table 5. The axial bond lengths of the An^{VI} crown complexes are slightly longer than those of the aquo species (by about 0.01 Å), indicating somewhat weaker bonds. For An^{V}, however, the bond lengths are almost identical in each case. Comparing next the equatorial bond lengths, we note that the distances are much shorter in the aquo complexes. The major part of this difference is due to the difference in equatorial coordination number: the aquo complexes have five oxygen donor atoms, and the crown complexes have six. For U^{VI}, we may include the six-coordinated aquo complex into the comparison as well. The change in equatorial bond lengths upon coordination of a sixth water molecule to $[UO_2(H_2O)_5]^{2+}$ is large indeed (0.06 Å).[37] However, the U−O(crown) bond lengths are still larger than the U−O(H_2) ones by about 0.04 Å, indicating weaker equatorial bonds for the crown system.

2. Actinyl Stretching Frequencies. We have calculated the harmonic vibrational (gas-phase) frequencies for all species considered in this work. The calculated actinyl stretching frequencies are shown in Tables 1−4.

Experimental vibrational frequencies are available only for the Np^{V} complex $[NpO_2(18\text{-crown-6})]^{1+}$. For this system, only the symmetric neptunyl stretching frequency has been measured experimentally and was found to be 780 cm^{-1}.

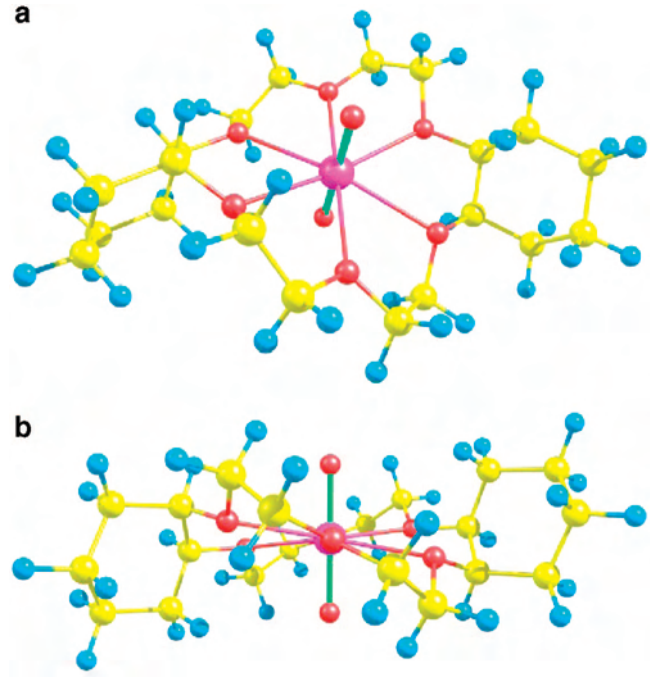

Figure 2. Optimized structure (AE/L2 PBE) of the uranyl complex formed with the bicyclohexyl-fused-crown, $[UO_2(\text{dicyclohexyl-18-crown-6})]^{2+}$, top (a) and side views (b).

The agreement between this value and the calculated numbers follows the trends for the calculated neptunyl bond lengths, as is generally the case for actinyl species, Table 3. The LC-ECP-B3LYP-calculated frequency is the closest to experimental results (absolute error 4 cm^{-1}), and this method results in the best neptunyl bond lengths, too. However this agreement must be considered fortuitous, as the result of substantial error cancellation: the LC-ECP scheme leads to underbinding, while the hybrid density functional B3LYP does overbind actinyl U−O bonds. The AE/L2-PBE approach yields a frequency of 791 cm^{-1}, with an absolute error of 11 cm^{-1}, as compared to experimental results. Of the methods studied, SC-ECP-B3LYP is furthest from experimental results, showing the strongest overbinding. While the preceding discussion focused on just one data point, the trend conforms to earlier observations for related systems:[37,38] Hybrid DFT methods like B3LYP always led to overbinding in the actinyl unit, as indicated by substantially overestimated vibrational frequencies, whereas GGA functionals such as PBE gave much better agreement to experimental results for both bond lengths and frequencies. Other aspects of the model chemistry, particularly the relativistic approximation, had only a modest influence on the frequencies, provided sufficiently converged basis sets had been used.[37,38] For the uranyl(VI) crown ether complex (Table 1), where we have done calculations using both the SC-ECP PBE and AE/L2 PBE methods, there is a good qualitative agreement between uranyl frequencies calculated by these methods. (We note that, for both these PBE calculations, the vibration corresponding to symmetric uranyl stretching accidentally couples with some of the crown ether vibrational modes, thus yielding two vibrational modes having strong contributions from the symmetric uranyl stretching component. In the table, we

Table 5. Priroda AE/L2 PBE Gas-Phase Results for for the Actinyl Penta-Aquo Complexes $[AnO_2(H_2O)_5]^{1+/2+}$, Recalculated from the Geometries in ref 37 with the Current Method's Settings (Bond Lengths in Å; Frequencies in cm^{-1})

	$[UO_2]^{2+}$	$[UO_2]^{1+}$	$[NpO_2]^{2+}$	$[NpO_2]^{1+}$	$[PuO_2]^{2+}$	$[PuO_2]^{1+}$
R An═O (axial)	1.768	1.817	1.748	1.799	1.738	1.786
	1.768	1.817	1.748	1.802	1.738	1.786
R An−O (equatorial)	2.473	2.586	2.468	2.586	2.468	2.572
	2.475	2.586	2.468	2.587	2.468	2.578
	2.485	2.586	2.470	2.587	2.468	2.584
	2.489	2.586	2.470	2.587	2.468	2.591
	2.497	2.588	2.472	2.587	2.468	2.594
average equatorial[a]	2.484	2.586	2.470	2.587	2.468	2.584
bond order An═O[b]	2.48	2.43	2.49	2.43	2.47	2.42
bond order An−O[c]	0.40	0.31	0.40	0.30	0.40	0.30
An charge	0.960	0.585	0.829	0.510	0.774	0.498
O charge	−0.238	−0.386	−0.205	−0.346	−0.165	−0.321
spin density on An	0.000	1.028	1.075	2.089	2.179	3.177
ν AnO_2 symm	892	817	888	809	866	801
ν AnO_2 asymm	979	873	985	884	981	885

[a] Arithmetic average. [b] Axial bond. [c] Equatorial bond.

Table 6. Charges (Hirshfeld), Spin Densities and Population Bond Orders in the Actinyl Unit $[AnO_2]^{n+}$ of the Respective Crown Ether Complexes (AE/L2-PBE Calculations)

complex $[AnO_2(18\text{-crown-}6)]^{n+}$	An charge	O charge	total AnO_2 charge	spin density on An	spin change $An^{VI}-An^{V}$	bond order An═O[a]	bond order An−O[b]
$[UO_2]^{2+}$	0.734	−0.263	0.208	0		2.46	0.34
$[UO_2]^{1+}$	0.498	−0.385	−0.272	1.030	1.030	2.42	0.24
$[NpO_2]^{2+}$	0.665	−0.233	0.199	1.099		2.46	0.34
$[NpO_2]^{1+}$	0.459	−0.349	−0.239	2.099	1.000	2.42	0.24
$[PuO_2]^{2+}$	0.610	−0.199	0.212	2.283		2.44	0.33
$[PuO_2]^{1+}$	0.416	−0.319	−0.222	3.190	0.907	2.41	0.23

[a] Axial (actinyl) bond. [b] Equatorial bond.

provide the calculated harmonic frequencies for both of them.)

The An^{VI} species have much higher actinyl frequencies than the respective An^{V} species, indicating stronger bonds. This is in accordance with the longer bond lengths for An^{V} as compared to An^{VI}, see above, and it is again in agreement with trends for other actinyl species.

If we compare, however, different actinide metals, we notice a trend of decreasing frequencies for An^{VI} (if going from U to Np to Pu). Thus, the bonds are decreasing in strength, despite the fact that they are decreasing in length also (see above). Indeed, both trends are due to the actinide contraction. The trend is not as pronounced for An^{V}.

Finally, comparing the respective crown and aquo complexes as calculated by the AE-PBE method (Table 5), we note that the latter have consistently higher actinyl stretching frequencies (and hence stronger bonds) than the former. Moreover, the difference is larger for the An^{VI} species than for An^{V}. All of that is consistent with the actinyl bond lengths, discussed before. Actinyl aquo complexes as well as bare actinyls show similar periodic trends in going from U to Np to Pu, that is, decreasing bond lengths and symmetric stretching frequencies, Table 5 and Table S1, Supporting Information.

3. Charges and Bond Orders. Metal and uranyl oxygen (Hirshfeld[57]) charges as well as population bond orders calculated with the AE/L2-PBE method are collected in Table 6. Partial charges as well as bond orders are nonobservable properties and, as such, not uniquely defined. This general problem has been discussed recently.[62,63] However, as pointed out above, our methods give results that agree well with simple chemical models for a wide range of actinide complexes.[27,38,59,60]

We notice that the absolute value of the positive charge on the metal, as well as the one of negative charges on actinyl oxygens, decreases along the actinide series for both An^{VI} and An^{V}. A substantial part of the charge is delocalized to the equatorial ligands (similar to the case of the penta-aquo complexes, Table 5). This is evident from the total charge on the AnO_2 fragment, which is substantially lower than its formal value of 2.0 or 1.0, respectively.

Upon reduction of An^{VI} to An^{V}, the extra electron goes entirely to the metal. This can be seen from the change in spin density upon reduction, Table 6. This behavior is in line with the penta-aquo complexes and bare actinyls, Table 5 and Table S1 (Supporting Information), but in contrast to our previous calculations on another group of macrocycles, expanded porphyrins, that form inclusion complexes with the actinyls, too. There, the electron is somewhat delocalized over the ligand, especially in the case of uranium. The delocalization was shown to decrease in a row U > Np > Pu.[27] The difference between these two types of systems can be understood from the nature of the ligand systems: the expanded porphyrin ligands possess extended conjugated π systems that allow for delocalization of the extra electron. Such systems are completely absent from the crown ethers or aquo complexes. The lowest unoccupied molecular orbitals in An^{VI} complexes are the 5f orbitals on the actinide metal that, in a purely ionic picture, would be completely nonbonding.

Actinyl bond orders are, in all cases, larger than two (in good agreement with the generally accepted view that these

(62) Clark, A. E.; Davidson, E. R. *J. Chem. Phys.* **2001**, *115*, 7382.

Table 7. Ligand Exchange and Complex Binding Energies Corresponding to Reactions 1−3 (kcal/mol)

	reaction*1*		reaction*2*		reaction*3*					
							$\Delta\Delta G_{solv}$ in water		ΔG in water[a]	
actinyl $[AnO_2]^{n+}$	ΔE	ΔG	ΔE	ΔG	ΔE	ΔG	CPCM	COSMO	CPCM	corrected COSMO[b]
					AE/L2-PBE (Priroda)					
$[UO_2]^{2+}$	−280.77	−259.99	−258.83	−204.14	−21.95	−55.85	32.07	22.33	−2.28	−12.02
$[UO_2]^{1+}$	−133.26	−114.51	−138.74	−86.49	5.48	−28.02	3.34[c]	−0.76[c]	−3.18 [c]	−7.29 [c]
$[NpO_2]^{2+}$	−272.89	−252.37	−251.63	−197.18	−21.26	−55.20	32.49	22.79	−1.21	−10.90
$[NpO_2]^{1+}$	−133.11	−114.76	−137.35	−84.84	4.24	−29.92	1.32	−2.58	−7.09	−11.00
$[PuO_2]^{2+}$	−273.28	−253.67	−250.60	−194.51	−22.67	−59.15	32.11	22.48	−5.55	−15.17
$[PuO_2]^{1+}$	−132.20	−113.79	−134.98	−82.90	2.79	−30.89	0.40	−3.18	−8.99	−12.57
					SC-ECP-B3LYP (G03)					
$[UO_2]^{2+}$	−284.58	−264.51	−274.63	−224.29	−9.96	−40.21	40.2	18.5	21.5	−0.2
$[UO_2]^{1+}$	−143.35	−124.80	−157.12	−106.01	13.78	−18.79	10.3	−5.9	13.0	−3.2
$[NpO_2]^{2+}$	−283.97	−264.31	−275.80	−223.15	−8.17	−41.16	40.7	18.6	21.0	−1.1
$[NpO_2]^{1+}$	−148.33	−130.12	−164.57	−113.04	16.24	−17.07	8.7	−6.4	13.1	−2.0
$[PuO_2]^{2+}$			−272.79	−220.08						
$[PuO_2]^{1+}$	−139.29	−121.02	−156.66	−105.05	17.37	−15.96	9.4	−7.6	14.9	−2.1

[a] $\Delta\Delta G^{solv}$ from G03 SC-ECP-B3LYP-CPCM calculations added; see the text. [b] Correction for translational entropy [5(4.3 kcal/mol)] of the five free waters on the right-hand side of eq 3 included.[56] [c] $[UO_2]^{1+}$•crown solvation energies were taken from corresponding $[NpO_2]^{1+}$ complexes; see the text.

bonds possess partial triple-bond character[1,2,51,64,65]) but decrease along the actinide series, despite decreasing bond lengths. This is again due to the actinide contraction, and it is in accordance with the discussion for the vibrational frequencies which also decrease with increasing atomic number. However, the corresponding An^{VI} and An^{V} species have calculated bond orders that are approximately equal in each case, in contrast to both the trend for the bare actinyl ions,[37] Table S1 (Supporting Information), and the trend in the vibrational frequencies, see above. As would be expected on the grounds of equatorial competition, the actinyl bond orders are smaller than those of the bare uranyl species[37] by 0.20 (U^{VI} and Pu^{VI}) and 0.18 (Np^{VI}) for the An^{VI} species and 0.12 to 0.13 for the An^{V} species, Table 6 and Table S1 (Supporting Information).

Equatorial bond orders are approximately 0.4 for the An^{VI} species but decrease to about 0.3 with the decrease of the cationic charge, that is, for An^{V}. In either case, the low bond orders are indicative of essentially ionic bonds in the equatorial plane. Such essentially ionic bonds fit the qualitative picture of the crown ether being a neutral aliphatic ligand with "hard" donor atoms (ether oxygens), and without anything as easily polarizable as, for example, a π system. This situation is again in contrast to complexes with alaskaphyrin and related expanded porphyrins where a similar bond order analysis revealed partial covalent character.[27,28]

4. Complex Stabilities. Choosing a suitable theoretical model for estimating complex stabilities is not a simple task since a whole range of (experimental) factors might influence it. Such factors include bulk solvation effects, counterions, acidity of the solutions, competing reactions, and so forth. The most straightforward quantity to analyze theoretically is the complex binding energy between a central atom or group (in our case, the actinyl ion) and a macrocyclic ligand. This corresponds to the Gibbs free energy ΔG for reaction 1

$$[AnO_2]^{n+} + (18\text{-crown-6}) \rightarrow [AnO_2(18\text{-crown-6})]^{n+} \quad (1)$$

However, the binding energy is not sufficient for estimating the complexing ability of the ligand—it has to be compared against the binding energy of the solvent complexes as well. In our case, these are the aquo complexes.[37]

$$[AnO_2]^{n+} + 5H_2O \rightarrow [AnO_2(H_2O)_5]^{n+} \quad (2)$$

Thus, a more realistic measure of complex stability might be the combination of reactions 1 and 2, that is, the ligand exchange reaction

$$[AnO_2(H_2O)_5]^{n+} + (18\text{-crown-6}) \rightarrow [AnO_2(18\text{-crown-6})]^{n+} + 5H_2O \quad (3)$$

These reactions, in particular, account for the relative stability of inner-sphere versus outer-sphere crown ether complexes. The latter are complexes in which the entire $[AnO_2(H_2O)_5]^{n+}$ species binds with one or two crown ethers to form an outer-sphere complex.[13] Reaction 3 can be applied in this respect, because, as a first approximation to the outer-sphere complex, the continuum-model solvated crown ligand can be used. Calculated electronic energies ΔE as well as Gibbs free energies ΔG for reactions 1−3 are shown in Table 7, for the methods we found to be most reliable above, that is, SC-ECP-B3LYP and AE/L2 PBE.

With respect to qualitative trends, both of these methods yield results consistent with each other: as to the absolute values, B3LYP, while overestimating the strength of ligand-to-actinyl binding as compared to the PBE (that is, it predicts lower energies of eqs 1 and 2), yields less exothermic/more endothermic values for the ligand exchange process eq 3. We note that both ΔE and ΔG are strongly negative for reactions 1 and 2, which can be considered as typical of gas-

(63) Clark, A. E.; Sonnenberg, J. L.; Hay, P. J.; Martin, R. L. *J. Chem. Phys.* **2004**, *121*, 2563.
(64) Denning, R. G. *Struct. Bonding (Berlin)* **1992**, *79*, 215.
(65) Denning, R. G.; Green, J. C.; Hutchings, T. E.; Dallera, C.; Tagliaferri, A.; Giara, K.; Brookes, N. B.; Braicovich, L. *J. Chem. Phys.* **2002**, *117*, 8008.

phase reactions involving charged species like bare metal ions, or actinyls in our case.

Next, we shall compare the binding energy of the crown ether ligand with that of five water molecules, reactions 1 versus 2. As should be expected from the known chemistry of actinyls, both the water and crown ether complexes of An^{V} show significantly lower binding energies than the complexes of An^{VI}. This can be related to the different charges on the actinyl unit, see above, and it should be expected for essentially ionic bonds. Furthermore, one can see that the electronic binding energies are higher in absolute values for the crown complexes of both An^{VI} and An^{V} than for the corresponding penta-aquo complexes.

The overall energy balance is reflected in the energies of reaction 3. It differs between the oxidation states: for An^{VI}, the crown complex formation from the penta-aquo complex is an energetically favorable process, while for An^{V} it is not. The Gibbs free energies of reaction eq 3 take into account entropy contributions to the effect of the reaction, in which five water molecules are released. This makes the ligand exchange from the penta-aquo to the crown ether complex favorable for both An^{V} and An^{VI}; still, for An^{V}, the process is much less exoergic than for An^{VI}. Therefore, the gas-phase calculations predict that the VI actinyls have a stronger affinity to crown ethers than the V actinyls, both in absolute terms, eq 1, and relative to aquo complexes, eq 3. This seems to contradict the experimental observations by Clark et al.,[17] namely, the existence of an in-cavity complex for $[NpO_2]^{1+}$ in aqueous solution, concurrent with the absence of a similar complex for the $[UO_2]^{2+}$ case. Indeed, Table 7 shows that the binding and ligand exchange energies do not differ dramatically between actinides in similar oxidation states—which means that the difference between the Np- and U-containing systems cannot be ascribed to the nature of the metal, either. Overall, the experimentally observed stabilization of the pentavalent oxidation state through crown ether complexation is not observed in the gas phase.

However, if we consider differences in solvation free energies for reaction 3 (provided in Table 7 as $\Delta\Delta G^{solv}$ in water), we see that there is a profound difference between the An^{V} and An^{VI} species. While for the former the values are highly positive (20–40 kcal/mol, depending on the choice of DFT method and solvation settings), for the latter, they are much less positive or even negative (again, depending on the method used).

This qualitative trend allows for an explanation of the experimental results. They are based entirely on differences in the relative solvation energies of the actinyl penta-aquo and crown complexes: For $[UO_2]^{2+}$, the aquo complex is solvated strongly by water, which makes the formation of in-cavity crown ether complexes unfavorable. At the same time, $[NpO_2]^{1+}$ is only weakly solvated by water, so it forms an inclusion complex, a process that is entropy-driven, as we have seen above.

Absolute values of the Gibbs free energy for the ligand exchange reaction are collected in the last two columns of Table 7. We note quite a large dependence of the results on the particular settings for the continuum model. The solvation energy changes $\Delta\Delta G_{solv}$ for B3LYP are also quite different from the ones calculated by PBE, which is easily understood because these methods yield slightly different geometries (thus different solvent-accessible surfaces) and charge distributions (with hybrid DFT giving structures that are more ionic and more highly charged than those from pure GGA methods.) It is well-known that changes in the model, particularly regarding the radii and the type of cavity surface used, might lead to changes in solvation energies up to 10 kcal/mol or so.[66] Here, we used two predefined sets of atomic radii—the standard united-atom model[39] as available in Gaussian 03 and the original COSMO radii by Klamt and Schüürmann.[55] We did not attempt to perform any optimizations for these radii. Thus, the absolute values might not be ideal in most cases; the best agreement for the combination of SC-ECP-B3LYP and COSMO could be just fortuitous. However, the qualitative trends are very clear and are independent of the model.

We have to note that our continuum model calculations, especially the settings concerning the model used (including only the first coordination sphere of the actinyls for both penta-aquo and crown ether complexes), yield results which are in agreement with the classical molecular dynamics (MD) simulations done by Wipff and Guilbaud[67,68] of the uranyl(VI) crown ether complex in water, where the solvent was modeled fully explicitly. Just as our continuum model calculations, these MD studies predicted that the uranyl crown ether complex is not stable in water; the uranyl would leave the ligand cavity during the simulation.

How could solvation be responsible for this stabilization of one particular oxidation state? As the leading effect, solvation stabilizes a charged solute by polarization of the polar solvent. The effect is proportional to the charge squared and inversely proportional to the distance between charge and polarizable medium. In reaction 3, the $n+$ charge is of course balanced. We notice, however, that $\Delta\Delta G^{solv}$ is in almost all cases positive. Moreover, depending on the model, $\Delta\Delta G^{solv}$ is several times larger for An^{VI} than for An^{V}, Table 7 (see above). Thus, solvation strongly destabilizes the right-hand side of reaction 3 relative to the left-hand side, and much more so for the actinyl(VI) dication than for the $1+$ charge of the actinyl(V) ion. This can be understood from the mentioned distance and charge dependence of the solvent–solute interactions: The size of the ligand system, and thus the distance between the charge (that is mostly concentrated on the actinyl ion) and the polarizable medium, is much larger for the crown ether complex than for the water complex. This leads to effective screening of the charge for the former relative to the latter. Because of the difference in charge, this effect is much more pronounced for An^{VI} than for An^{V}, leading to the relative stabilization of the actinyl(V) crown ether complexes.

(66) Rotzinger, F. P. *Chem. Rev.* **2005**, *105*, 2003.
(67) Guilbaud, P.; Wipff, G. *J. Phys. Chem.* **1993**, *97*, 5685.
(68) Guilbaud, P.; Wipff, G. *THEOCHEM* **1996**, *366*, 55.

Conclusions

In this article, we have used modern relativistic DFT to study the inclusion complexes formed between the 18-crown-6 macrocycle and the actinyl ions $[AnO_2]^{n+}$, $n = 1$ and 2 and An = U, Np, and Pu. We get good agreement—similar in quality to earlier results for various other systems[27,28,37,38,60] —between the calculated and experimental geometries and vibrational frequencies. This is particularly true for the neptunyl(V) complex where accurate experimental results are available.[17] However, the large experimental uncertainties all but preclude such conclusions for the uranyl(VI) complexes.[15,16] Overall, we have confidence in the predictive power of our methods. Consequently, we have used them to predict the structures, vibrational frequencies, and other properties of all six complexes, including the experimentally unknown species such as the plutonium complexes.

The axial (actinyl) bonds were found to have partial triple-bond character, in accordance with the generally accepted view of these bonds.[1,2,64,65] The bond orders decrease slightly along the actinide series in going from U to Np to Pu, whereas stretching frequencies and bond lengths decrease more strongly. These trends can be associated with the actinide contraction. Upon reduction of the actinyl(VI) complex to the corresponding actinyl(V) complex, we find that the extra electron is located at the central actinide metal. This can be understood from the aliphatic nature of the crown ether ligand. It is in contrast to the case of expanded porphyrin systems[27] where the aromatic ring system of the ligand allows for a certain degree of delocalization of the extra spin density in An^V complexes.

The complex stability has been studied by calculating the Gibbs free energy for ligand exchange reaction 3 (exchange of five waters for the crown ether ligand). Perhaps the most interesting question in this connection is the reason for the experimentally observed stabilization of the pentavalent oxidation state by ring systems such as the crown ethers. It has been speculated[69] that this stabilization comes about because "*reduction from oxidation state VI to V gives an expanded metal ion radius that provides a better fit to the* [ligand] *cavity*." Our calculations do not support this assertion. Indeed, if the fit/misfit criteria were the reason for the stabilization of the pentavalent oxidation state, then we should see the effect in the gas phase as well as in solution. This is, however, not the case, and it is solely in solution that we reproduce the stabilization of the pentavalent relative to the hexavalent oxidation state. Thus, we propose that solvation in a polar solvent is the reason for the effect. We have also provided a qualitative explanation: The positive charge of the actinyl unit is more effectively screened from the polarizable solvent by the large macrocycle (as compared to the aquo ligands), leading to positive free energies of solvation for reaction 3, $\Delta\Delta G_{solv}$, Table 7, that is, a relative destablization of the inclusion complex in solution. This effect is much more pronounced for the large 2+ charge of the hexavalent oxidation state than for the 1+ charge of the pentavalent ions, leading to the *relative* stabilization of the $[AnO_2(18\text{-crown-}6)]^{1+}$ complexes.

Acknowledgment. We are grateful to D. N. Laikov for making his Priroda code available to us and for technical advice. We thank D. L. Clark, Los Alamos, for inspiring discussion in the initial stages of this work. G.A.S. and G.S. acknowledge financial support from the Natural Sciences and Engineering Research Council of Canada (NSERC) and from the University of Manitoba (startup funds and University of Manitoba Research Grants Program). R.L.M. and P.J.H. acknowledge support from the LANL Laboratory Directed Research and Development Program and the Division of Chemical Sciences, Office of Basic Energy Sciences, Heavy Element Chemistry program. This work was carried out under the auspices of the National Nuclear Security Administration of the U.S. Department of Energy at Los Alamos National Laboratory under Contract No. DE-AC52-06NA25396.

Supporting Information Available: Full citation for ref 39; properties of bare actinyl cations $[AnO_2]^{1+/2+}$ (Table S1); calculated Priroda AE/L2 PBE gas-phase total electronic energies, thermodynamic functions, and G03-PBE calculated single-point solvation energies (Table S2). This material is available free of charge via the Internet at http://pubs.acs.org.

IC7015403

(69) By an unknown reviewer to a related paper.